Thermotopes-COH—A software for carbon isotope modeling and speciation of COH fluids

COMPUTERS & GEOSCIENCES
VOL. 184
ISSN 0098-3004
DOI: 10.1016/j.cageo.2024.105533

Thermotopes-COH — a software for carbon isotope modeling and speciation of COH fluids

Antoine Boutier[1,2,3]*, Isabelle Martinez[3], Isabelle Daniel[2], Simone Tumiati[4], Guillaume Siron[5], Alberto Vitale Brovarone[5,6,7]

[1]*Dipartimento di Scienze della Terra, Università degli Studi di Torino, Via Valperga Caluso 35, 10100 Torino, Italy, ORCID: 0000-0003-4013-0566*

[2]*Université de Lyon, Univ Lyon 1, ENS de Lyon, CNRS UMR 5276, LGL-TPE, Villeurbanne Cedex, France*

[3]*Université Paris Cité, Institut de Physique du Globe de Paris, CNRS, UMR 7154, F-75005, Paris, France.*

[4]*Dipartimento di Scienze della Terra, Università degli Studi di Milano, via Mangiagalli 34, I-20133, Milano, Italy*

[5]*Dipartimento di Scienze Biologiche, Geologiche e Ambientali, Via Zamboni, 67, Bologna, Italy*

[6]*Institut de Minéralogie, de Physique des Matériaux et de Cosmochimie (IMPMC), Sorbonne Université, Muséum National d'Histoire Naturelle, UMR CNRS 7590, IRD UR206, 75005 Paris, France*

[7]*Institute of Geosciences and Earth Resources, National Research Council of Italy, Pisa, Italy*

*Corresponding authors: antoine.boutier@gmail.com; alberto.vitaleb@unibo.it

Authorship Statement:

Category 1:

Conception and design of study: Antoine Boutier, Alberto Vitale Brovarone

Coding: Antoine Boutier

Concept and features consultation: Simone Tumiati, Guillaume Siron.

Category 2:

Drafting the manuscript: Antoine Boutier, Alberto Vitale Brovarone.

Revising the manuscript critically for important intellectual content: Isabelle Martinez, Isabelle Daniel, Simone Tumiati, Guillaume Siron.

Category 3:

Approval of the version of the manuscript to be published: Antoine Boutier, Alberto Vitale Brovarone, Isabelle Martinez, Isabelle Daniel, Simone Tumiati, Guillaume Siron.

Abstract

Carbon-bearing fluids and condensed carbon are common on and inside planetary bodies. Understanding the mechanisms capable of transferring carbon from fluids into solids and vice-versa is central in many fundamental and applied research targets within the Earth and Planetary Sciences. A broad range of applications can benefit from the thermodynamic properties of carbon-oxygen-hydrogen (COH) systems. As an example, the precipitation of natural graphite or diamond can be modeled within the COH thermodynamic systems. Because the evolution of COH fluids implies isotopic fractionation among different species, carbon stable isotopes can be used in conjunction with thermodynamic calculations to reconstruct graphite or diamond formation mechanisms, or the evolution of fluid species such as carbon dioxide or methane.

Thermotopes-COH is a Python-based graphical user interface (GUI) software for computation of thermodynamic and carbon isotopic modeling in the C-O-H system within the 0.1 – 5 GPa and 300 – 900 °C range. The software allows generic and process-oriented thermodynamic and carbon stable isotope calculations including fluid mixing, fluid-graphite/diamond interactions with changing pressure or temperature, and fluid desiccation. This versatile numerical tool is designed to model processes of dissolution/precipitation of graphite or diamond. Along with a description of the software functions, this contribution also provides practical examples.

Keywords: Carbon, Isotopes, COH-fluid, Modeling, Thermodynamics

1 Introduction

Carbon cycling on Earth is pivotal in bridging biological and geological processes, energy fluxes in both shallow and deep environments, and climatic and global environmental changes (Berner, 1999; Dasgupta, 2013; Dasgupta and Hirschmann, 2010; Evans, 2011). Carbon is ubiquitous in geologic fluids, e.g., in hydrocarbon-rich fluids, as small fractions in aqueous fluids or dominant in CO_2-rich systems (Connolly and Cesare, 1993; Huang et al., 2017; Kokh et al., 2017). Carbon isotope geochemistry has long been used to track sources and processes in geologic systems (Baumgartner and Valley, 2001; Bebout and Fogel, 1992; Duke and Rumble, 1986; Kitchen and Valley, 1995; Luque et al., 2012; Mason et al., 2017; Ray, 2009; Ray and Ramesh, 2000; Stachel et al., 2017; Tumiati et al., 2022; Valley, 1986).

Carbon also is a redox-sensitive element, and its isotopic evolution strongly depends on the thermodynamic evolution of the geologic system under consideration. The COH thermodynamic system has long been used to model the evolution of many geological fluids and fluid-rock systems as a function of pressure (*P*), temperature (*T*), and redox state. Some examples include the study of graphite or diamond precipitation from carbon-saturated/supersaturated fluids, graphite dissolution in response to regional metamorphism or fluid infiltration, and the subsequent speciation in fluid inclusions (Cesare, 1995; Connolly, 1995; Connolly and Cesare, 1993; French, 1966; Ohmoto and Kerrick, 1977; Taylor and Liou, 1978; Taylor and Green, 1986; Ulmer and Luth, 1991; Huizenga 2005; Galvez et al., 2013; Vitale Brovarone et al., 2020).

The thermodynamics of the COH system has also been used to reconstruct the carbon isotopic evolution of graphite or diamond precipitation at carbon saturation conditions (Duke and Rumble, 1986; Stachel et al., 2017; Ortega et al., 2010; Boutier et al., 2023). While the

77 relations governing the chemical equilibria of the COH system and its isotopes exist (Duke and
78 Rumble, 1986, Holloway, 1984; Huizenga, 2005; Spycher and Reed, 1988; Rumble and
79 Hoering, 1986), their integration into a single, user-friendly software is not yet available.
80 Furthermore, when complex fluid or fluid/rock evolutions are considered within the COH
81 system, the isotopic trend of the resulting fluid and solid phases may be challenging to model
82 or even counterintuitive (Stachel et al., 2017).

83 Although numerical tools allowing computation of simple isotope equilibria exist (e.g.,
84 Beaudoin and Therrien, 2009, 2004), the computations are often done using user-made,
85 specific spreadsheets. The Thermotopes-COH software integrates carbon isotope and
86 thermodynamic models allowing for complex fluid and fluid-rock reactions and interactions
87 within the COH chemical system. It features multiple functions through five interactive tabs:
88 (1) carbon isotopic equilibrium, (2) carbon isotopic fractionation modeling, (3) multi-
89 component solid-C precipitation, (4) COH fluid speciation, and (5) graphite/diamond
90 dissolution/precipitation. The core of Thermotopes-COH provides advanced tools to model
91 the thermodynamic and isotopic evolution of fluids and their interactions with
92 graphite/diamond-bearing rocks within the COH chemical system. The software offers generic
93 and process-oriented modeling options spanning the most common mechanisms of
94 graphite/diamond precipitation or dissolution and a fast graphical visualization of the
95 modeling results. The software also offers the possibility to perform conventional calculations
96 such as carbon isotopic equilibria and fractionation modeling for further use as internal input
97 parameters for the more advanced options.

98 This Python-based software runs on Windows and MacOS. It is a standalone executable that
99 does not require any additional installation of packages. The software and documentation are

available at https://zenodo.org/record/8364254. This contribution presents the software functions and principles, as well as examples of applications of its functionalities.

2 Isotope and thermodynamic database

2.1 Isotope database

Isotope fractionation equations can be presented under various form, with the most comprehensive as follow:

$$\Delta = 1000\ ln\ \alpha = A\frac{(10^{3n})}{T^n} + \cdots + D\frac{(10^6)}{T^2} + E\frac{(10^3)}{T} + F \quad (1)$$

where Δ is the isotopic fractionation, α is the fractionation factor, *A* to *F* are experimentally determined parameters and T is temperature in K.

Since the higher order terms have been recognized to contribute insignificantly to isotopic fractionation between two phases (Richet et al., 1977), the isotopic database of Thermotopes-COH uses a simplified version of the general equation limited to the second power:

$$\Delta = 1000 ln\alpha = A\frac{(10^6)}{T^2} + B\frac{(10^3)}{T} + C \quad (2)$$

This model includes a wide range of available references in the COH system but may limit the implementation of additional fractionation factors containing higher order terms. The full list of fractionation factors featured in the carbon isotopic database used in Thermotopes-COH is presented in Table 1.

120 Table 1: List of fractionation factor available in Thermotopes-COH

Isotopic Couple	Temperature range	Reference
CO_2-CH_4	0-700°C	Bottinga,Y. (1969)
Graphite-CH_4	0-700°C	Bottinga,Y. (1969)
Calcite-CH_4	0-700°C	Bottinga,Y. (1969)
Calcite-Aragonite	25°C	Rubinson,M. and Clayton,R.N.(1969)
Diamond-Graphite	0-1000°C	Bottinga,Y. (1969)
Calcite-CO_2	100-700°C	Bottinga,Y. (1969)
		Bottinga,Y. (1968)
	0-100°C	Deines,P.; Langmuir,D.; and Harmon,R.S. (1974)
	900°C	Rosenbaum,J.M. (1994)
	0-600°C	Ohmoto,H.; and Rye,R.O. (1979)
Calcite-Graphite	0-700°C	Bottinga,Y. (1969)
	400-800°C	Dunn,S.R. and Valley,J.W. (1992)
	400-680°C	Wada,H. & Suzuki,K. (1983)
	600-1200°C	Scheele,N. & Hoefs,J. (1992)
	700-800°C	Kitchen,N.E. & Valley,J.W. (1995)
	600-1400°C	Deines,P., Eggler,D.H (2009)
CO_2-Graphite	100-700°C	Bottinga,Y. (1969)
	0-1000°C	Bottinga,Y. (1969)
Diamond-CO_2		Bottinga,Y. (1969)
Diamond-CH_4		Bottinga,Y. (1969)
Dolomite-CO_2		Ohmoto,H.; and Rye,R.O. (1979)
Calcite-HCO_3	0-100 °C	Deines,P. et al. (1974)
CO-CO_2	0-330 °C	Ohmoto,H. & Rye,R.O. (1979)

121

2.2 Thermodynamic database

The thermodynamic calculations in the Thermotopes-COH software follow the COH model by Huizenga (2005) based on the numerous equations of state available allowing a wide range of initial input parameters. The thermodynamic data for solids are taken from Shi and Saxena (1992). The list of considered oxygen fugacity buffers is presented in Table 2. The thermodynamic dataset for diamond/graphite is from Day (2012).

Table 2: List of oxygen fugacity buffers available in Thermotopes-COH

Oxygen fugacity buffer	Reference
FMQ	Miozzi & Tumiati (2020)
(Fayalite-Magnetite-Quartz)	O'Neill (1987) and Ballhaus et al. (1991)
	Ohmoto & Kerrick (1977)
Hem-Mag	Ballhaus et al. (1991)
(Hematite-Magnetite)	Frost (1991)
Fe-Wus	Ballhaus et al. (1991)
(Iron-Wustite)	Frost (1991)
Ni-NiO	Ballhaus et al. (1991)
	Frost (1991)
EMOD	Stagno and Frost (2010)
(Enstatite-Magnesite-Olivine-Diamond/Graphite)	

3 Thermotopes-COH structure and functions

This section presents the modeling functions of Thermotopes-COH, their assumptions, and some practical examples. The Thermotopes-COH GUI displays five different tabs. The first three tabs are designed to obtain input parameters for the following ones. The tabs called "Isotopic equilibrium" and "Isotopic fractionation", respectively, provide isotopic input parameters at desired conditions, including simple isotope equilibria and open/closed system isotope fractionation. The third tab, called "Multicomponent solid-C" provides a first coupling of COH thermodynamics and isotope evolution for multi-component, carbon-saturated systems. The fourth tab, called "COH system" is centered on the thermodynamics of the COH system and provides carbon isotope evolution for fluid and solid species. The fifth tab, called "Dissolution/precipitation", provides process-oriented integration of thermodynamic and isotope evolutions of fluid species and condensed carbon minerals (graphite/diamond).

3.1 Isotopic equilibrium

The tab labeled "Isotopic equilibrium" is the basic building block of Thermotopes-COH. It calculates isotopic equilibrium between two carbon-bearing species, using the following expression:

$$\delta_A = \delta_B + \Delta_{A-B} \quad (3)$$

where δ_A is the isotopic composition of A in per mille (‰), δ_B is the isotopic composition of B in permil (‰), Δ_{A-B} is the isotopic shift between A and B calculated after Eq.(2) (Kendall and McDonnell, 2012; Sharp, 2017). The list of isotopic couples available in this tab is shown in Table 1.

3.2 Isotopic fractionation

The tab labeled “Isotopic fractionation” calculates batch or Rayleigh fractionation evolutions of a C-bearing species. Isotopic fractionation between species A to B is calculated at equilibrium. Batch (or closed system) fractionation is derived from mass balance equation (Valley, 1986):

$$\delta_B^f = \left(\delta_A^{initial} - \Delta_{A-B}\right) \times (1 - f) + \left(\delta_A^{initial} \times f\right) \quad (4)$$

$$\delta_A^f = \delta_B^f + \Delta_{A-B} \quad (5)$$

Rayleigh (or open system) fractionation follows the so-called Rayleigh equation (Rayleigh, 1896):

$$\delta_A^f = ((1000 + \delta_A^{initial}) f^{\alpha_{A-B}-1}) - 1000 \quad (6)$$

$$\delta_B^f = \frac{(1000+\delta_A^f)}{\alpha_{A-B}} - 1000 \quad (7)$$

where f is the remaining fraction of A, $\delta_A^{initial}$ is the initial isotopic composition at the beginning of the fractionation, δ_A^f and δ_B^f are the isotopic composition at f, and α_{A-B} is the fractionation factor calculated after Eq.(2) (Dansgaard, 1964; Kendall and McDonnell, 2012; Sharp, 2017; Valley, 1986).

Figure 1 shows two examples of modeling outputs for the isotope fractionation of graphite to either CO_2 or CH_4 in closed or open system conditions, at 300 °C and 500 °C. This example provides a quick visualization of the effect of temperature on the fractionation factor of the graphite-CO_2 and graphite-CH_4 couples. It shows, for example, that the temperature effect is more important for the graphite-CH_4 couple. This behavior has an important role in the isotopic evolution of multi-component systems described in the next section.

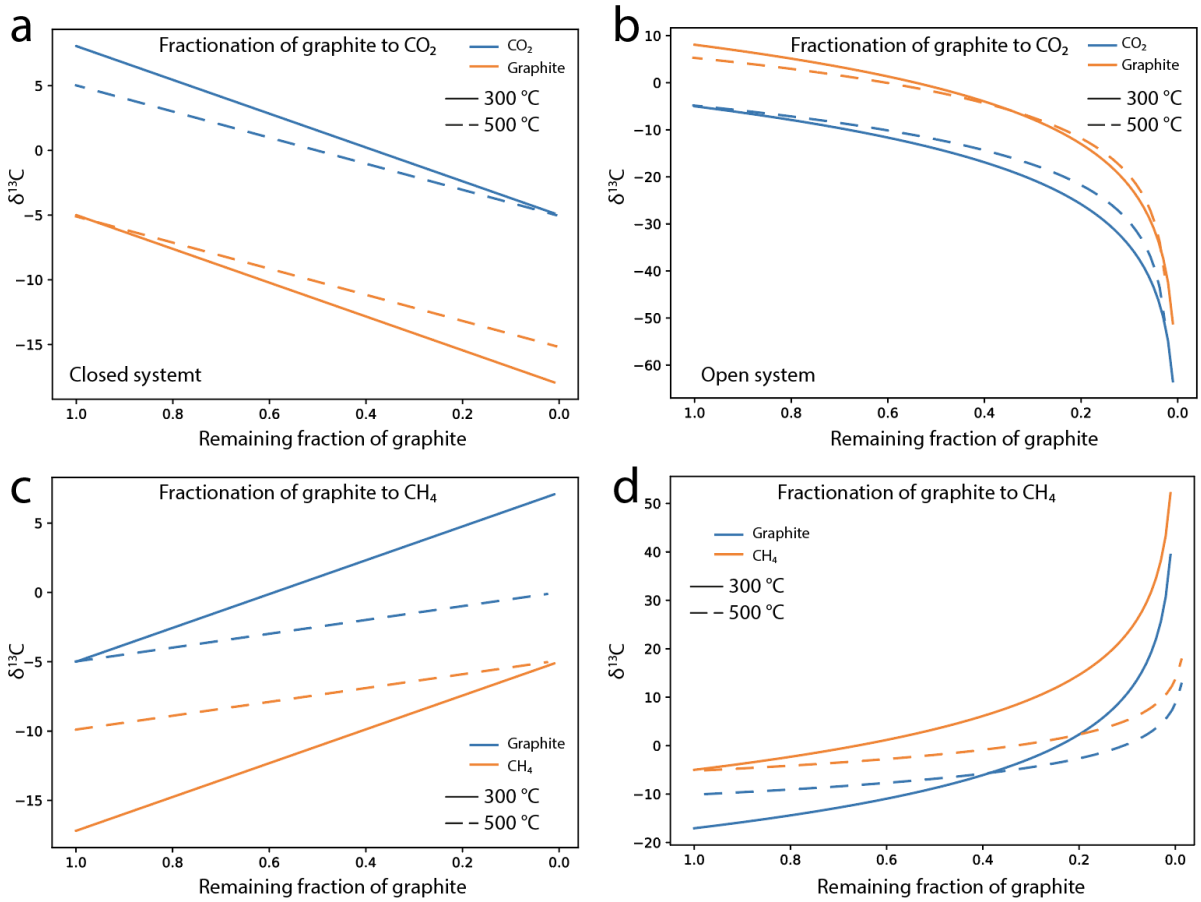

174

175 Figure 1. Examples of closed (a, c) and open (b, d) system fractionation of graphite to either CO_2 (a, b) or CH_4 (c,
176 d). Each panel shows fractionation evolution at 300 (solid line) and 500 °C (dashed line), respectively. The
177 software allows to easily select a source and a product and to model their isotopic evolution as a function of the
178 remaining fraction of the source at a given temperature. All species and fractionation factor available in the
179 software are given in Table 1.

180 ## 3.3 Multi-component graphite/diamond-CO_2-CH_4 modeling

181 The tab labeled “Multi-component solid-C'' models the precipitation of either graphite or
182 diamond, from a fluid containing both CO_2 and CH_4 according to the equation described
183 successively by Ray (2009), Ray and Ramesh (2000), and by Stachel et al. (2017). The
184 precipitation of graphite/diamond from a fluid containing both CO_2 and CH_4 follows two steps:
185 initially, and as long as available, CO_2 and CH_4 contribute equally to the isotopic value of the
186 resulting C_{solid} (0.5 mole each per mole of produced graphite/diamond). Then, when the less

abundant phase either CH_4 or CO_2 is totally consumed, precipitation evolves as a single component system following a classical Rayleigh model (see Tab 2). During the first step, the equations (12) and (17) defining the isotopic value of C_{solid} varies if the system is CH_4 or CO_2 dominated (Ray, 2009; Ray and Ramesh, 2000; Stachel et al., 2017b). When CH_4 is more abundant than CO_2 the equations are:

$$\delta^{13}C_{fluid}^{f} = 1000\left(\frac{\alpha_{C-CH4}}{A} ln\frac{Af-B}{A-B} - lnf\right) + \delta^{13}C_{fluid}^{initial} \quad (8)$$

$$\delta^{13}C_{C\ solid}^{f} = 1000\left(\frac{\alpha_{C-CH4}}{A-\frac{B}{f}} - 1\right) + \delta^{13}C_{fluid}^{f}\left(\frac{\alpha_{C-CH4}}{A-\frac{B}{f}}\right) \quad (9)$$

$$r = \frac{XCO_2}{XCH_4} \quad (10)$$

$$A = \frac{1+\alpha_{CO2-CH4}}{2} \quad (11)$$

$$B = (1-r)\frac{\alpha_{CO2-CH4}-1}{2+2^r} \quad (12)$$

When CO_2 is more abundant than CH_4:

$$\delta^{13}C_{fluid}^{f} = 1000\left(\frac{\alpha_{C-CO2}}{A} ln\frac{Af-B}{A-B} - lnf\right) + \delta^{13}C_{fluid}^{initial} \quad (13)$$

$$\delta^{13}C_{C\ solid}^{f} = 1000\left(\frac{\alpha_{C-CO2}}{A-\frac{B}{f}} - 1\right) + \delta^{13}C_{fluid}^{f}\left(\frac{\alpha_{C-CO2}}{A-\frac{B}{f}}\right) \quad (14)$$

$$r = \frac{XCH_4}{XCO_2} \quad (15)$$

$$A = \frac{1+\frac{1}{\alpha_{CO2-CH4}}}{2} \quad (16)$$

$$B = (1-r)\frac{\alpha_{CO2-CH4}}{2+2^r} \quad (17)$$

where $\delta^{13}C_{fluid}^{initial}$ is the initial isotopic composition of the fluid, $\delta^{13}C_{fluid}^{f}$ the isotopic composition of the fluid for a remaining fraction of fluid *f*, $\delta^{13}C_{C\ solid}^{f}$ is the composition of graphite/diamond at the remaining fraction of fluid *f*, $\alpha_{CO2-CH4}$ the fractionation factor

between CO_2 and CH_4, α_{C-CO2} the fractionation factor between graphite/diamond and CO_2 and α_{C-CH4} the fractionation factor between graphite/diamond and CH_4.

Multi-component isotope calculations are performed by selecting an option for the input of $\delta^{13}C$ isotopic composition of the fluid, either "Total C", "Fluid mixing", "Known CH_4 composition" or "Known CO_2 composition".

-Total C: The fluid is considered in internal isotopic equilibrium and the total $\delta^{13}C$ value of the fluid is entered. The isotopic compositions of CO_2 and CH_4 are then calculated based on their respective proportion at the desired temperature.

-Fluid mixing: Two fluids initially at isotopic disequilibrium contain either CO_2 or CH_4. Once the precipitation starts, the two fluids mix to reach isotopic equilibrium and then ensue the precipitation of graphite/diamond.

-Known CH_4 (or CO_2) composition: The fluid is at isotopic equilibrium but only the $\delta^{13}C$ CH_4 (or CO_2) composition is known by the user. In this case, software will models the associated missing $\delta^{13}C$ composition at the desired temperature and derives the precipitation of graphite/diamond.

Please note that the modeling of graphite/diamond precipitation from the tab "Multi-component G/D-C-O-H modeling" does not involve thermodynamic computations. Nevertheless, the isotopic mass balance used for the multi-component modeling follows the same principles of evolving COH speciation as those that define the thermodynamic modeling presented in section 3.4.

Figure 2 shows two examples of multi-component graphite precipitation models for CH_4/CO_2 ratios >1 and <1, respectively, at 300 °C and 500 °C. The initial bulk $\delta^{13}C$ is -5‰ in both cases. The evolution of single component systems for either CH_4 or pure CO_2 is also shown for comparison. As observed by Stachel et al. (2017), the evolution of multi-component systems may result in counterintuitive trends. In Figure 2, it can be observed that, depending on the initial CH_4/CO_2 ratio, the coexisting fluid and graphite follow consistent (CH_4/CO_2 ratio < 1) or opposite trends (CH_4/CO_2 ratio > 1), because $\Delta_{graphite\text{-}CH4}$ is smaller than $\Delta_{graphite\text{-}CO2}$. This results in a progressive enrichment in ^{13}C in the precipitating graphite and a progressive enrichment in X_{CH4} (and therefore a depletion in ^{13}C in the remaining fluid) for fluid with CH_4/CO_2 ratio > 1, or a progressive enrichment in both ^{13}C in the precipitating graphite and X_{CO2} for fluid with CH_4/CO_2 ratio < 1. Depending on the temperature conditions, the fluid and graphite isotopic trends do or do not cross each other (Figure 2). This is the result of the multi-component evolution, when the fluid and precipitating solid may transiently have the same $\delta^{13}C$ composition. Such a feature is generally observed for a complete transformation in a closed reservoir (for example, full transformation of CO_2 to graphite), whereas in the present case it is observed for transient open-system conditions. As introduced in the previous section, the diversity in temperature dependence between the graphite-CO_2 and graphite-CH_4 couples determines remarkable variations in the isotopic fractionation of the precipitating graphite, especially for CH_4/CO_2 ratios >1. In particular, at 300 °C for a CH_4/CO_2 ratio >1, the first precipitating graphite is enriched in ^{13}C relative to the fluid source, whereas at 500 °C the first precipitating graphite is depleted in ^{13}C relative to the fluid source. This is due to the difference between $\Delta_{graphite\text{-}CH4}$ and $\Delta_{graphite\text{-}CO2}$ that decreases with increasing temperature. In other words, $\Delta_{CH4\text{-}CO2}$ decreases with increasing temperature but with more substantial variations for the CH_4-graphite pair. Although $\Delta_{graphite\text{-}CH4}$ remains smaller than $\Delta_{graphite\text{-}CO2}$ with

increasing temperature, the decreasing $\Delta_{CH4\text{-}CO2}$ with increasing temperature determines, for a fixed CH_4/CO_2 ratio > 1, that the first precipitating graphite is enriched in ^{13}C relative to the fluid source at low temperature, whereas it is depleted in ^{13}C relative to the fluid source at higher temperature. The successive fractionation trends are controlled by the evolving CH_4/CO_2 ratio as described above.

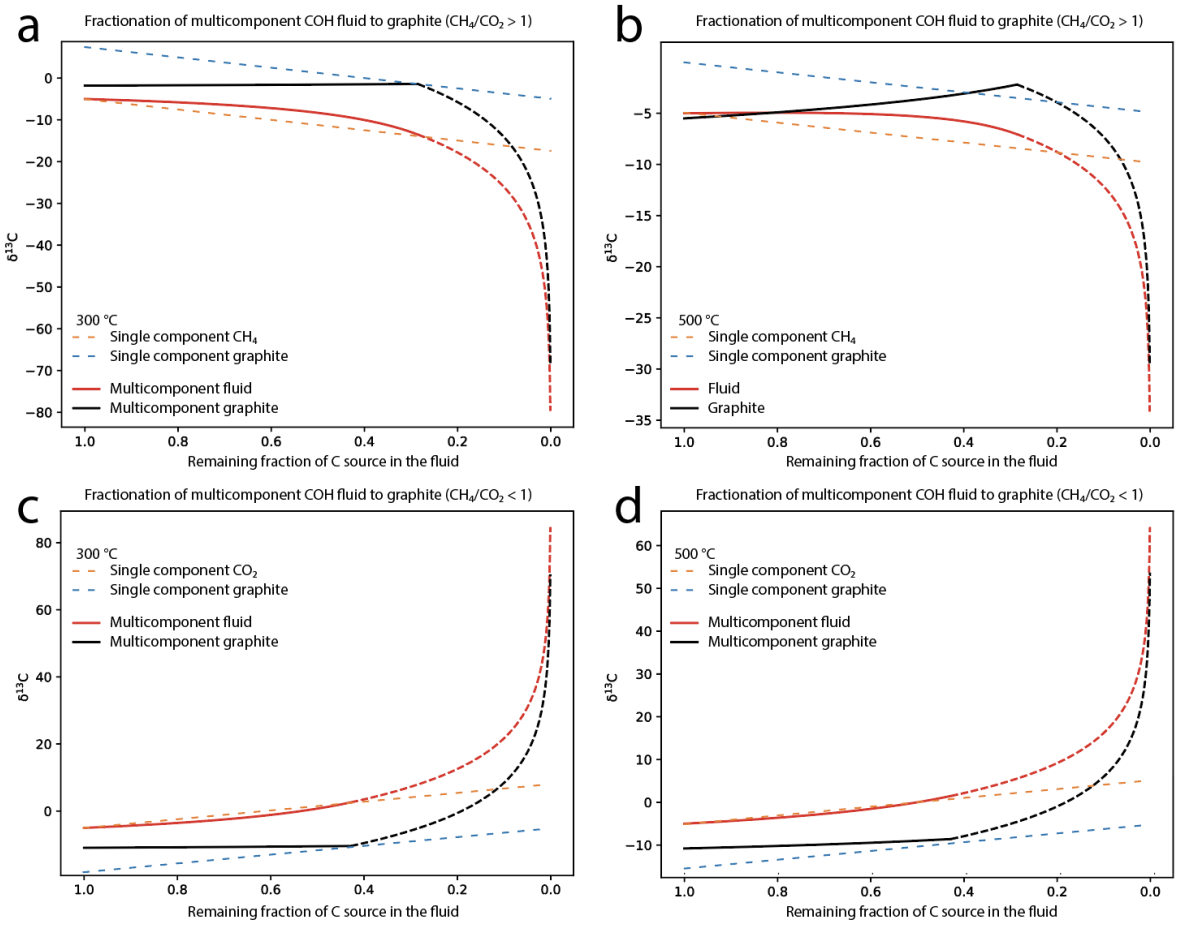

Figure 2. Examples of multi-component isotope fractionation trends for CH_4/CO_2= 1.8 (CH_4 0.64; CO_2 0.36) at 300 °C (a) and 500 °C (b) and CH_4/CO_2 = 0.4 (CH_4 0.29; CO_2 0.71) at 300 °C (c) and 500 °C (d), for initial $\delta^{13}C$ = -5 ‰. SIngle component fractionations are also shown for reference. The system firstly evolves as multi-component (solid lines) until the less abundant molecule –CO_2 in (a,b), CH_4 in (c,d)– is exhausted. Secondly, it evolves as a single-component system (dashed lines).

3.4 COH fluid speciation

The tab labeled "COH system" models the speciation of COH fluids, the carbon activity, the X_O, and the oxygen and hydrogen fugacities. The modeling follows equations from Huizenga (2005) and references therein, and calculates the speciation of the COH fluid using the following equilibria:

$$CO + \frac{1}{2}O_2 = CO_2 \quad (18)$$

$$H_2 + \frac{1}{2}O_2 = H_2O \quad (19)$$

$$CH_4 + 2\,O_2 = CO_2 + 2\,H_2O \quad (20)$$

$$C_{solid} + O_2 = CO_2 \quad (21)$$

From these equilibria, the oxygen fugacity f_{O_2} along with the molar fractions of X_{H_2O}, X_{CO_2}, X_{CH_4}, X_{H_2} and X_{CO}, are calculated. X_O is defined as $X_O = \frac{n_O}{n_O + n_H}$ where n_O and n_H are the atomic proportions of oxygen and hydrogen in the fluid, respectively (Connolly and Cesare, 1993).

The model assumes ideal mixing. Details of the equation for the equilibrium constants of reaction and fugacity coefficients can be found in Huizenga (2005) and reference therein.

f_{H_2} is calculated according to the following equation (Holloway, 1977):

$$f_{H_2} = \gamma_{H_2} \times P \times X_{H_2} \quad (22)$$

Where X_{H_2} is the molar fraction of H_2, P is the pressure in bar, and γ_{H_2} is the fugacity coefficient of hydrogen calculated following Huizenga (2005). The carbon activity is the effective concentration of carbon in the fluid. A carbon activity of 1 indicates that the fluid is saturated in carbon and coexists with graphite/diamond. Carbon activity above to 1 refers to a carbon oversaturated fluid or to the equilibrium with a non-ideal (e.g., disordered) carbon

form (Tumiati et al., 2020; Vitale Brovarone et al., 2020), which is not integrated in the current version of the software. Carbon activity lower than one refers to graphite/diamond-undersaturated conditions.

Several modeling options are available that require either 2 or 3 input parameters among:

- known carbon activity, f_{O_2} buffer, and a Δ log f_{O_2} from this buffer
- known carbon activity and $XCO_2/(XCO_2 + XCH_4)$ ratio. A f_{O_2} buffer can be indicated for reference.
- known $XCO_2/(XCO_2 + XCH_4)$ ratio, f_{O_2} buffer, and a Δ log f_{O_2} from this buffer
- known carbon activity and X_O. A f_{O_2} buffer can be indicated for reference.
- known $XCO_2/(XCO_2 + XCH_4)$ ratio and XH_2O. A f_{O_2} buffer can be indicated for reference.

The Δ log f_{O_2} correspond to the relative difference to the selected oxygen fugacity buffer. For example, for a fluid at ΔFMQ+1 (log units), Δ log f_{O_2} value is 1.

The results can be visualized on a ternary COH diagram (Fig. 3). The latter displays the location of the carbon saturation curve and the position of the modeled COH fluid composition. The software also allows expanding the computations over a pressure-temperature range and to plot them on a P-T diagram (Fig. 4).

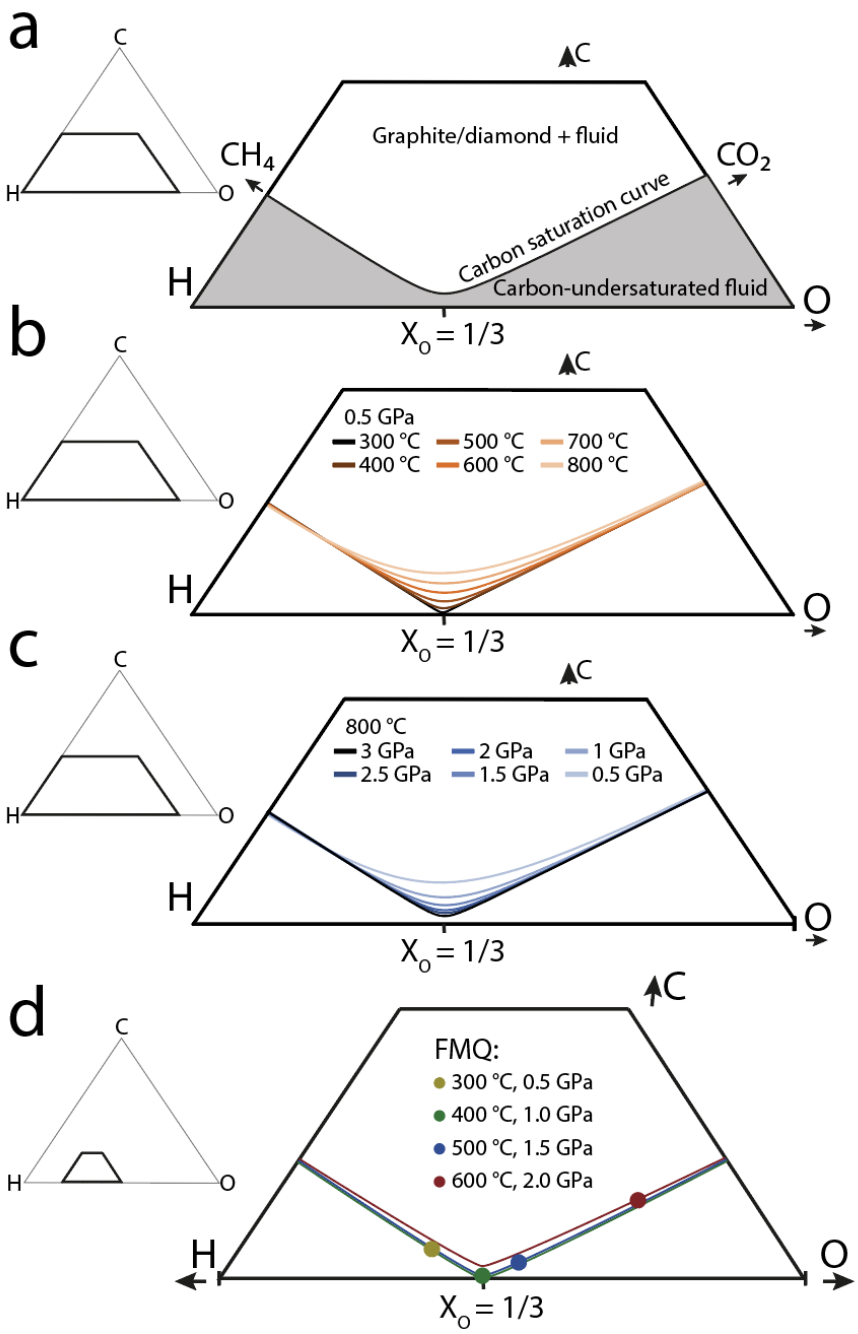

299

300 Figure 3. (a) Example of ternary COH diagram showing a generic carbon saturation curve separating the field of
301 carbon-undersaturated fluids from the field where the fluid coexists with graphite/diamond. (b-d) Ternary COH
302 diagrams showing the position of the carbon saturation curve for different temperatures and constant pressure
303 (b), for different pressures at constant temperature (c), and along a prograde metamorphic path highlighting
304 the positions of the FMQ buffer for four pressure-temperatures couples (d). FMQ buffer from Miozzi and Tumiati
305 (2020).

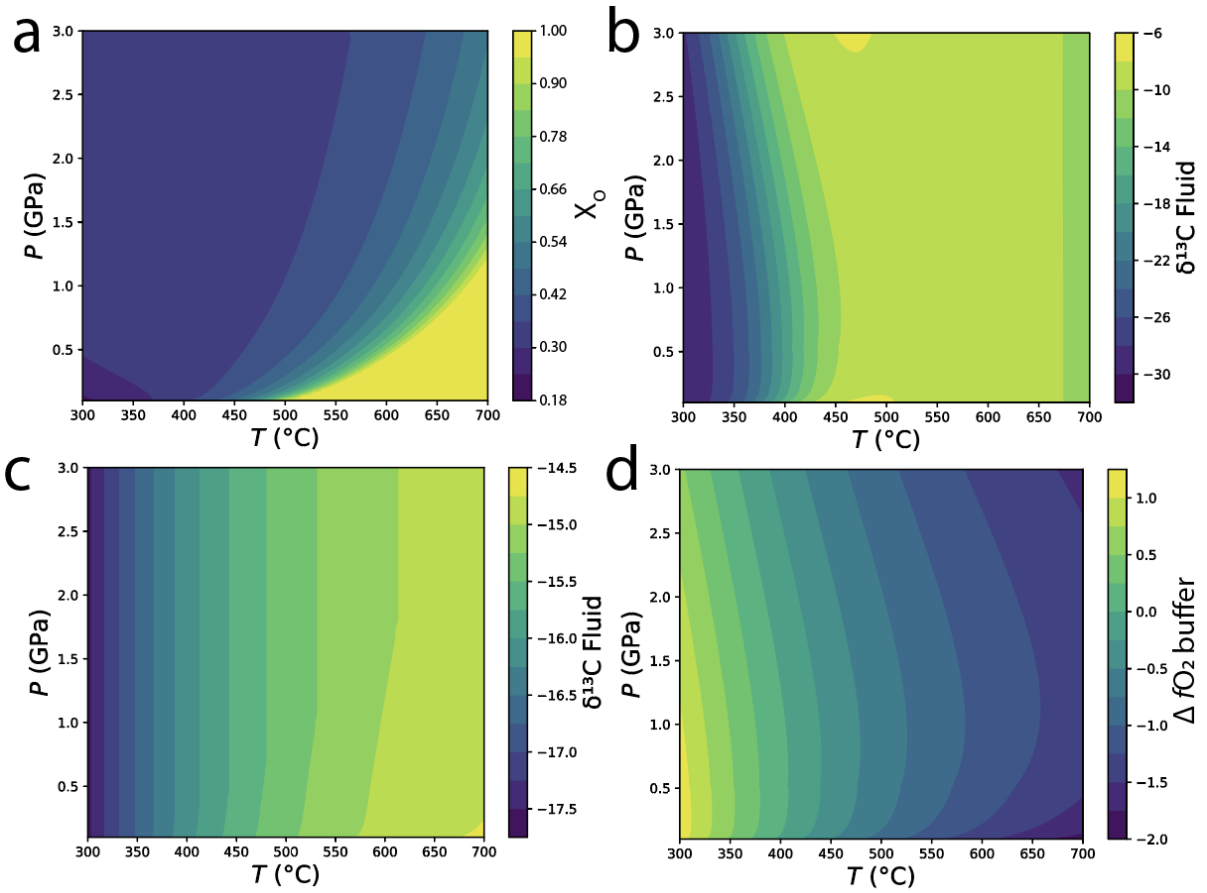

306

307 Figure 4. (a) X_O colormap for a graphite saturated fluid at FMQ. (b) $\delta^{13}C$ colormap of a carbon-saturated fluid in
308 equilibrium with graphite/diamond ($\delta^{13}C$ graphite = -18 ‰), at FMQ. (c) $\delta^{13}C$ colormap of a carbon-saturated
309 fluid in equilibrium with graphite/diamond ($\delta^{13}C$ graphite = -18 ‰), at water-maximum conditions (X_O = ⅓). (d)
310 ΔlogFMQ colormap for a carbon-saturated fluid at water maximum (X_O = ⅓).

311 ### 3.4.1 Application to the study of carbon-saturated fluid inclusions

312 A potential application of the COH system tab is for the post entrapment fluid-component re-
313 speciation in carbon-saturated fluid inclusions. Cesare (1995) described the transformation of
314 graphite-saturated fluid inclusions during cooling and decompression. Provided that no mass
315 is gained or lost by the inclusions, the original X_O ratio of the fluid phase should be constant
316 (Cesare, 1995). Because the position of the carbon saturation curve within the COH diagram
317 is dependent upon P and T conditions, cooling and/or decompression drive variations in fO_2
318 and carbon content of the fluid, which in turn leads to the precipitation of graphite inside the

inclusions. As a consequence, carbon speciation changes inside the fluid phase of the inclusions. By compiling results for a series of P-T couples, Cesare (1995) concluded that the $CO_2/(CO_2 + CH_4)$ ratio increases during cooling for fluids with initial XO > ⅓, whereas it decreases for fluids with initial XO < ⅓. The P-T graph option of the COH system tab of Thermotopes-COH offers the possibility to plot the $CO_2/(CO_2 + CH_4)$ ratio of graphite-saturated fluids for constant X_O values and to assess the carbon speciation in the fluid along any cooling and decompression path (Fig. 5). The fO_2 variation can also be plotted. If a fixed composition for the initial graphite in equilibrium with the trapped fluid is set, the software allows the calculation of P-T diagrams of $\delta^{13}C$ values for the bulk fluid, CH_4, or CO_2. Since these diagrams assume a constant isotopic value for the graphite in equilibrium with the fluid inclusion, the $\delta^{13}C$ values across a P-T diagram generated through the COH tab do not take into account any isotopic mass balance during the precipitation of graphite inside the inclusions with decreasing pressure and temperature, which would induce isotopic fractionation of the remaining fluid. For this reason, it is not recommended to use boldly the $\delta^{13}C$ results of the COH tab to track the isotopic evolution of fluid inclusions during pressure and temperature variations unless the assumption is made that the solid carbon precipitated inside the inclusion does reequilibrate isotopically after its formation. A way to overcome this issue consists in considering a $\delta^{13}C$ equal to 0‰ for the graphite coexisting with the fluid. This way, the P-T diagrams for carbon isotopes represent directly the Δ between the fluid phases (bulk, CO_2, or CH_4) and the solid inside the inclusion.

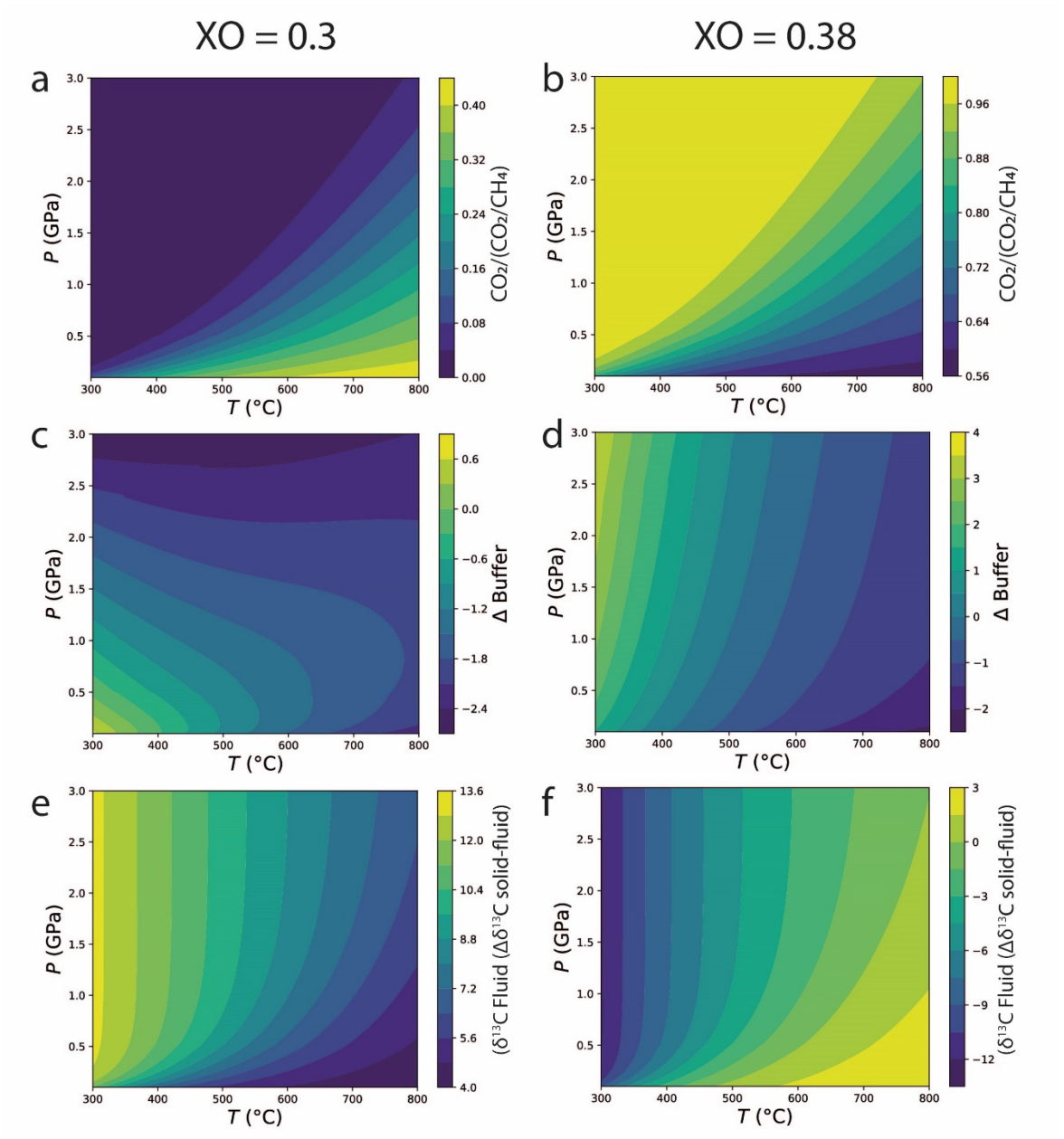

339

340 Figure 5. Pressure-temperature diagrams for the carbon-saturated COH system. In (a) and (b), fixed X_O values of
341 0.3 and 0.38 are considered as representative of more reduced and more oxidized conditions, respectively,
342 relative to the water-maximum conditions (X_O = ⅓). The ΔLogFMQ for both X_O values is also shown in (c) and (d),
343 respectively. Panels (e) and (f) show the $\delta^{13}C$ evolution of the bulk fluid (CH_4+CO_2). As explained in the text, these
344 values across the P-T space refer to a constant $\delta^{13}C$ for the solid carbon in equilibrium with the fluid. These
345 diagrams were constructed for a $\delta^{13}C$ value of solid carbon at 0‰, so that, at any point within the diagram, the
346 $\delta^{13}C$ value directly refers to the $\Delta\delta^{13}C$ between the solid and the bulk fluid.

3.5 Dissolution/precipitation of graphite/diamond

The tab labeled “Dissolution/precipitation”, offers process-oriented solutions to investigate the precipitation and/or dissolution of graphite/diamond. The model assumes equilibrium conditions and tracks the carbon activity of a COH-fluid through various reactions according to the equations in Huizenga (2005). In short, graphite/diamond precipitation is obtained for any fluid evolution resulting in carbon activity higher than 1, or when a carbon-saturated fluid evolves along the carbon saturation curve from H_2O richer to H_2O poorer compositions. Graphite/diamond dissolution is observed when the fluid evolves from carbon-saturated conditions to carbon undersaturated conditions, or when a fluid evolves from H_2O poorer to H_2O richer compositions along the carbon saturation curve. The governing equilibrium is:

$$CH_4 + CO_2 \leftrightarrows\ 2\,H_2O + 2\,C_{solid} \qquad (23)$$

The respective isotopic composition of the solid and fluid is calculated along the reaction path according to reaction (23).

Since graphite/diamond may behave as a chemically reactive but isotopically inert phase (Tumiati et al., 2022; Valley and O’Neil, 1981), an option is provided to allow graphite/diamond to participate in the isotopic mass balance. When this option is toggled on, the initial and newly formed graphite/diamond in the system can freely equilibrate with other C-bearing species in the system and participate in the mass balance. The isotopic system is considered to be closed, with carbon being either in the fluid phase or as graphite/diamond. The composition of solid-C is calculated through the following equation:

$$\delta^{13}C_{solid} = \delta^{13}C_{system} - \frac{nCO_2}{nC_{total}}\Delta_{CO2-C} - \frac{nCH_4}{nC_{total}}\Delta_{CH4-C} \qquad (24)$$

with $\delta^{13}C_{solid}$ being the isotopic composition of solid-C, $\delta^{13}C_{system}$ the isotopic composition of the system, $n\mathrm{CO_2}$ and $n\mathrm{CH_4}$ the number of moles of $\mathrm{CO_2}$ and $\mathrm{CH_4}$, respectively, $n\mathrm{C}_{total}$ the total number of moles of carbon in the system Δ_{CO2-C} and Δ_{CH4-C} the isotopic capital delta between $\mathrm{CO_2}$ and graphite/diamond and $\mathrm{CH_4}$ and graphite/diamond, respectively.

When this option is toggled off, graphite/diamond in the system does not participate in the isotopic mass balance unless a fraction of this solid-C is dissolved. In this case, the isotopic composition of the newly formed graphite/diamond is calculated considering the instantaneous remaining fraction of carbon in the fluid *f* as follows:

$$f = 1 - \left(\frac{nC_{solid\,new}}{nCH_4 + nCO_2}\right) \qquad (25)$$

The isotopic compositions of the instantaneous graphite/diamond and the total graphite/diamond are then calculated from a combination of equation (4) and an isotopic mass balance. A comparison of the isotopic calculation between the multicomponent system and the Dissolution/precipitation model is presented in Supplementary material 1.

Thermotopes-COH offers six conceptual models for graphite/diamond dissolution/precipitation, which are presented hereafter.

3.5.1 Dissolution/precipitation of graphite/diamond during fluid mixing

The fluid mixing process models the interaction of two different COH-fluids and their resulting potential to dissolve or precipitate graphite/diamond. The software models the titration of the second fluid into the first one through an iterative process. The titration step is defined as 0.1% of the second fluid being mixed in the first one. The carbon activity of the fluid is calculated and, if a_C=1, the titration proceeds to the next step. If the carbon activity is either > 1 or < 1, a sub-iteration starts with either dissolution or precipitation of graphite/diamond

until the carbon activity reaches 1. The associated isotopic evolution of fluid species and graphite/diamond is computed at each step. The titration proceeds until the totality of the second fluid is mixed within the first one.

Figure 6 shows examples of models involving the mixing of 100 moles of reduced graphite-saturated fluid into 100 moles of a more oxidized one, at 500 °C and 1 GPa. The host fluid has a $CO_2/(CO_2 + CH_4)$ ratio of 0.95, corresponding fO_2 values equivalent to the FMQ buffer, and is in equilibrium with graphite with $\delta^{13}C$ = -30 ‰, which corresponds to a $\delta^{13}C$ value of -20.6 for the fluid. The second fluid has a $CO_2/(CO_2 + CH_4)$ ratio of 1.9×10^{-4}, corresponding to ΔLogFMQ = -3, and is in equilibrium with graphite with $\delta^{13}C$ of -5 ‰, which corresponds to a $\delta^{13}C$ of -34.9 ‰ for the fluid. Two examples are considered, with either inert or exchanging graphite in the host system (1 mole graphite), respectively. The amount of graphite precipitation, the fO_2 evolution, and the fluid component speciation are equivalent in both cases, and characterized by the precipitation of about 31 moles of graphite, a decrease of the fO_2 of about 3 log units, and by an increase of the $CH_4/(CH_4 + CO_2)$ ratio from nearly 0 in the host fluid, to about 1 in the mixed fluid. The $\delta^{13}C$ of the system, however, is different in the two cases. The isotopic exchange of the host graphite (-30 ‰) results in a decrease of the $\delta^{13}C$ of CO_2 and increase of the $\delta^{13}C$ of CH_4.

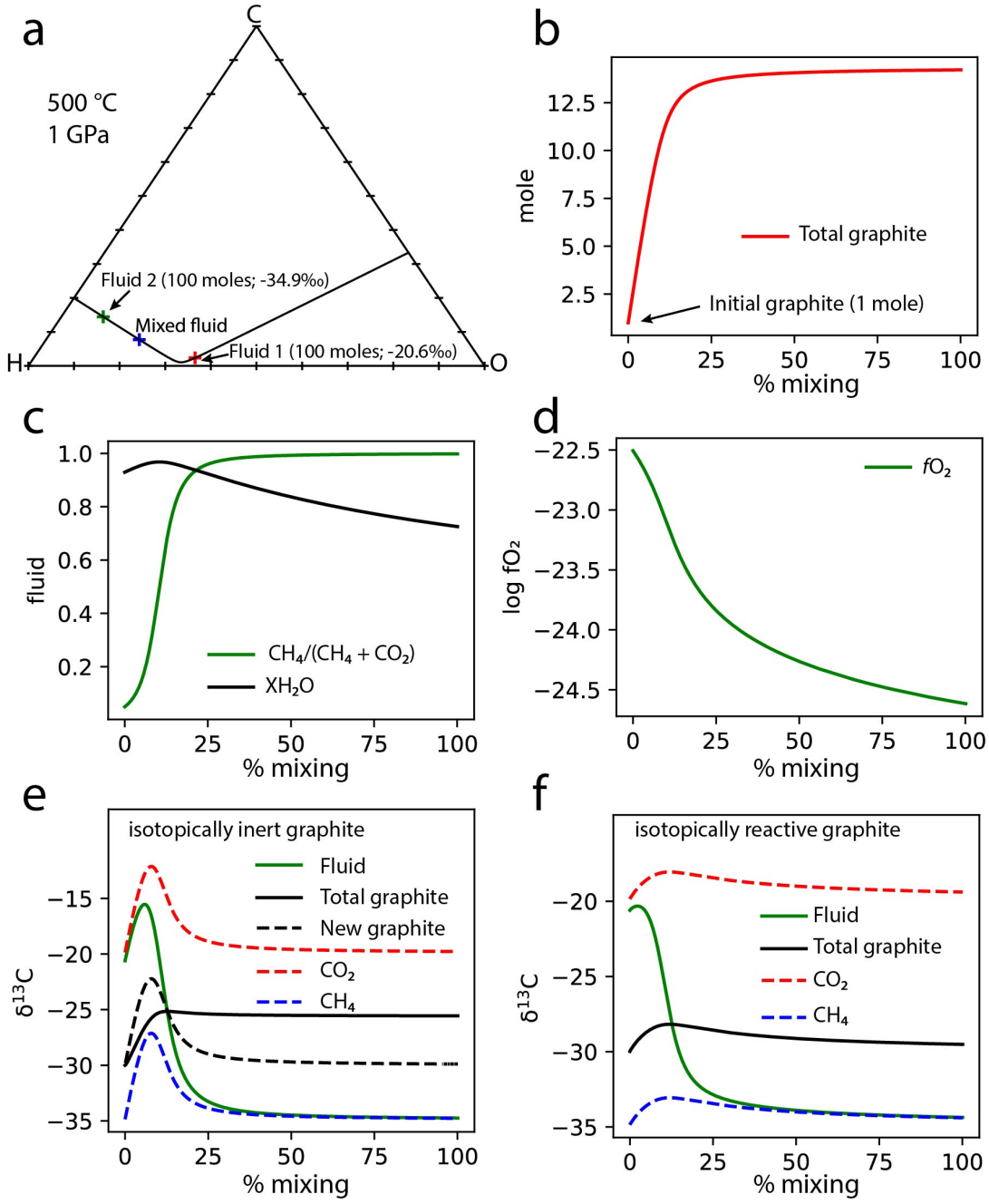

407

408 Figure 6. Examples of graphite precipitation through fluid mixing. Panel (a) shows the position of the two mixing
409 fluids (both carbon-saturated) and the final one. Panel (b) shows the number of moles of graphite precipitated
410 due to mixing. Panel (c) shows the evolution of the $CH_4/(CH_4 + CO_2)$ ratio and XH_2O and (d) of the fO_2 during the
411 mixing, respectively. Panels (e) and (f) show the $\delta^{13}C$ of the solid, the bulk fluid, CO_2, and CH_4 during the mixing
412 for isotopically inert (e) and isotopically exchanging (f) initial solid. The mixing of 100 moles of fluid 1 with 100
413 moles of fluid 2 was calculated at 500 °C, and for a preexisting graphite with $\delta^{13}C$ = -30‰.

In these examples, it can be observed that the mixing of two carbon-saturated fluids may lead to transient, counterintuitive trends in the carbon isotope evolution of both the fluid species and the precipitated graphite. This includes isotopic values transiently heavier than the heaviest fluid being involved in the mixing. This effect is due to the evolution of the mixing in a complex multi-component (CO_2 + CH_4) system across the water-maximum: an initially CO_2-dominated fractionation trend, followed by a CH_4-dominated one, and a contextual precipitation of variable amounts of graphite during the mixing.

The software also offers the possibility to model fluid mixing at buffered f_{O_2}conditions. This option models the interaction of a fluid with an f_{O_2} buffer, to simulate interaction in a buffered medium. The f_{O_2} is Δlog relative to a list of buffers (e.g., FMQ or EMOG), fixed during the whole process, and the software models the composition of an external fluid equilibrating with a constant f_{O_2}. If graphite/diamond precipitates, its isotopic composition is also calculated. Geologically, buffering the f_{O_2} is not a trivial assumption and should be selected only if consistent with the natural or experimental conditions.

3.5.2 Desiccation

This interaction models the evolution of a desiccating COH fluid (e.g., through rock hydration reaction, or respeciation of H and O into C-bearing fluid species) and calculates the associated precipitation of graphite/diamond. The desiccation is here defined as the loss of H_2O moles from the initial fluid. In the desiccation mode, the oxygen fugacity is free to evolve during the desiccation. During fluid desiccation, the carbon concentration increases and, if carbon saturation is reached, graphite/diamond precipitates. The degree of desiccation that is entered, corresponds to the fraction of the water loss (X_{H_2O}). The model is iterative and, at each step, 0.01% of the moles of the initial H_2O ($n H_2O$) is removed, the carbon activity is

calculated, and the number of moles of precipitated graphite/diamond and its isotopic value are derived. The calculation proceeds until the desired water fraction of the initial fluid is lost. Figure 7 shows desiccation of a fluid slightly oxidized relative to the water maximum at 600 °C and 0.5 GPa (ΔLogFMQ = -0.5, Fig. 7a) . The $\delta^{13}C$ of the fluid was set at -10‰, and the desiccation rate could proceed to 100%. Figure 7b shows that, during the desiccation of the chosen carbon-saturated COH fluid, graphite is constantly precipitated during a progressive increase in fO_2. Despite the desiccation ratio being set to 100%, the final fluid still contains some water (Fig. 7c). This water is produced in response to graphite/diamond precipitation and is not accounted for by the desiccation process. The newly formed water remains in the fluid. At the chosen high temperature conditions, the $\delta^{13}C$ of the precipitating graphite shows minimal variations during the desiccation process. As introduced in the previous section, lower temperatures should increase the range of $\delta^{13}C$ values in an evolving carbon-saturated COH fluid.

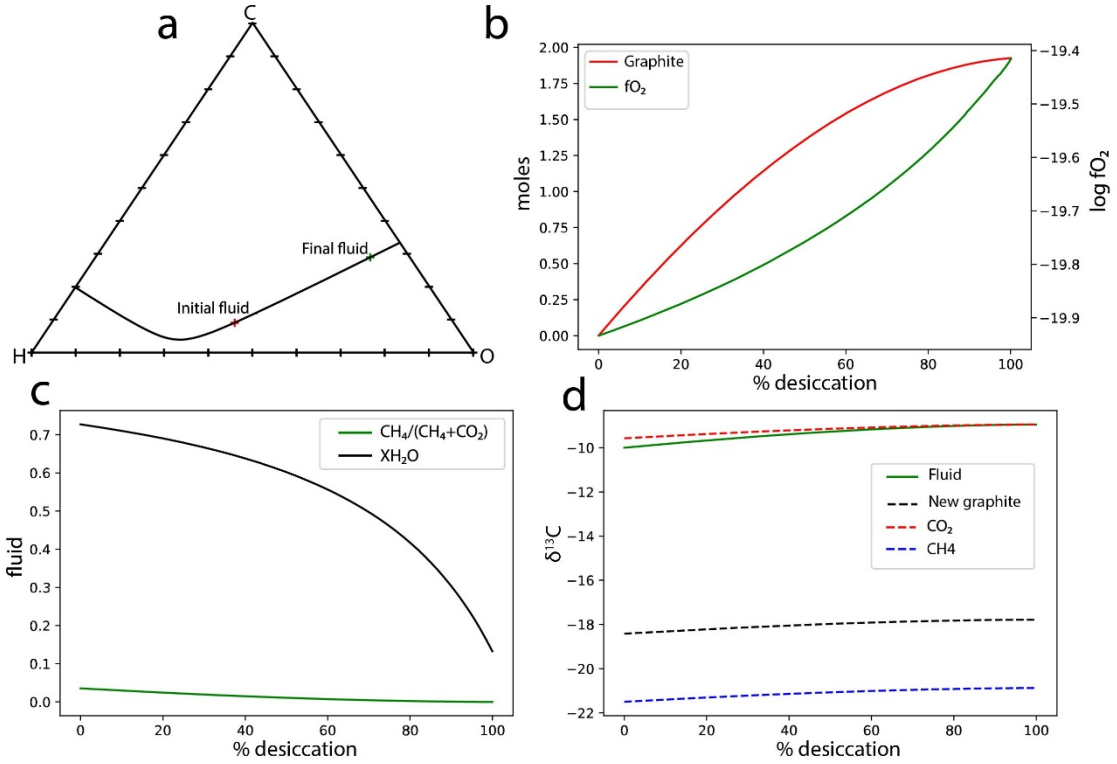

Figure 7. Desiccation model at 600 °C and 0.5 GPa. The $\delta^{13}C$ of the fluid was set at -10‰, and the fO_2 at ΔLogFMQ = -0.5. Desiccation ratio was 100%. A: COH diagram showing the position of the fluid prior to the interaction and its final position after graphite precipitation. B: Evolution of graphite precipitation in response to changing fO_2 during desiccation. C: H_2O and $CH_4/(CH_4 + CO_2)$ proportions during desiccation. D: Isotopic composition of the fluid, of its C-bearing species CO_2 and CH_4, and of graphite formed in response to fluid desiccation.

Also, the desiccation option can be modeled at buffered f_{O_2} conditions. The desiccation is here defined as the loss of H_2O mole in the fluid, and because the f_{O_2} is fixed during the interaction, the water fraction in the fluid remains constant while the fluid stays at carbon saturation. In other words, the actual amount of water decreases rather than its molar fraction. Any loss of H_2O is accompanied by the loss of an equivalent amount of the other species in the fluid in order to maintain X_{H_2O} constant. The amount of desiccation must be entered, because redox conditions are buffered, X_{H_2O} remains constant during desiccation. If graphite/diamond precipitates, its isotopic composition is also calculated. Geologically speaking, buffering f_{O_2} is not a trivial assumption and this option should be used with caution. This option is probably better suited to experimental rather than natural conditions.

3.5.3 Pressure change

The “pressure change” option models the evolution of a COH fluid at equilibrium undergoing isothermal pressure changes. The model is iterative. At each pressure step (every 0.01 GPa), the thermodynamic parameters of the COH system are calculated. If graphite/diamond is dissolved/precipitated, its isotopic composition is calculated.

3.5.4 Temperature change

The “temperature change” option models the evolution of an equilibrium COH fluid undergoing isobaric thermal changes. The model is iterative. At each temperature (every 1 °C), the thermodynamic parameters of the COH system are calculated. In the event of graphite/diamond is dissolved/precipitated, its isotopic composition is calculated.

4 Limitations

Maximum temperature and pressure:

The equation of state Thermotopes-COH software limits the applicable pressure-temperature range to crustal and upper mantle geological conditions and may react poorly in eclogitic or granulitic conditions. Thermodynamic equations from Huizenga, (2005) cover the range above 300°C and 0.1 GPa. Pairs of P-T values in proximity of the extremes of the allowed range may lead to unexpected results or errors.

Pure CO_2 or CH_4 fluid

At temperatures higher than ≈ 850 °C, the composition of carbon saturated fluids tends towards pure CO_2 and CH_4 becomes virtually absent. Conversely, should the user force overwhelmingly reduced conditions featuring only pure CH_4 fluid, the COH system will be left to the CH system. In the endmember situations, mathematical errors may arise from ratios leading to division by zero. In this event, the software will inform the user that the modeling cannot be pursued due to fluid being pure CO_2 or CH_4.

Graphite/diamond precipitation

493 Graphite/diamond precipitation is based on Equation (23) (see Section 2.7) as the sole
494 precipitation reaction. More reactions could be considered, as the model strays from reality
495 when only CO_2 or CH_4 remains present in the fluid, such as equation (21) involving oxidation
496 of graphite/diamond in CO_2.

497

498 5 Acknowledgment

499 Isotopic parameters come mainly from a compilation of isotopic fractionation equations from
500 "IsoFrac" Jordi Delgado Martin. This work is part of a project funded by the European
501 Research Council (ERC) under the European Union's Horizon 2020 research and innovation
502 program (Grant agreement No. 864045; project acronym DeepSeep). A Richard Lounsbery
503 grant and a MIUR Rita Levi Montalcini grant to AVB are also acknowledged.

504 6 Computer code availability

505 The Thermotopes-COH software was developed by Antoine Boutier, (Dipartimento di Scienze
506 della Terra, Università degli Studi di Torino, Via Valperga Caluso 35, 10100 Torino
507 antoine.boutier@gmail.com, +33-644255635), under the supervision of Alberto Vitale
508 Brovarone (Dipertimento di Scienze Biologiche, Geologiche e Ambientali, Università di
509 Bologna, Piazza di Porta San Donato 1, 40126 Bologna; alberto.vitaleb@unibo.it).The source
510 codes and user manual are available at https://zenodo.org/record/8364254 under an open
511 source license. The software is compatible with current Microsoft operating system Windows
512 10, and Apple Mac operating system (tested on Mojave and Catalina), and is written in
513 Python, using Python 3.7.2. The software code makes use of the freely available package

Matplotlib, Tkinter and Pandas, and has been compiled using Pyinstaller with Windows PowerShell.

7 References

Ballhaus, C., Berry, R.F., Green, D.H., 1991. High pressure experimental calibration of the olivine-orthopyroxene-spinel oxygen geobarometer: implications for the oxidation state of the upper mantle. Contrib. Mineral. Petrol. 107, 27–40.

Baumgartner, L.P., Valley, J.W., 2001. Stable isotope transport and contact metamorphic fluid flow. Rev. Mineral. Geochem. 43, 415–467.

Beaudoin, G., Therrien, P., 2009. The updated web stable isotope fractionation calculator. Handb. Stable Isot. Anal. Tech. 2, 1120–1122.

Bebout, G.E., Fogel, M.L., 1992. Nitrogen-isotope compositions of metasedimentary rocks in the Catalina Schist, California: implications for metamorphic devolatilization history. Geochim. Cosmochim. Acta 56, 2839–2849.

Berner, R.A., 1999. A new look at the long-term carbon cycle. Gsa Today 9, 1–6.

Boutier, A., Martinez, I., Sissmann, O., Agostini, S., Daniel, I., Van Baalen, M., Mana, S. and Brovarone, A.V., 2023. Complexity of graphite formation in response to metamorphic methane generation and transformation in an orogenic ultramafic body. Geochimica et Cosmochimica Acta.

Cesare, B., 1995. Graphite precipitation in C—O—H fluid inclusions: closed system compositional and density changes, and thermobarometric implications. Contrib. Mineral. Petrol. 122, 25–33.

Connolly, J.A.D., 1995. Phase diagram methods for graphitic rocks and application to the system C-O- H- FeO- TiO 2- SiO 2. Contrib. Mineral. Petrol. 119, 94–116.

Connolly, J.A.D., Cesare, B., 1993. C-O-H-S fluid composition and oxygen fugacity in graphitic metapelites. J. Metamorph. Geol. 11, 379–388.

Dansgaard, W., 1964. Stable isotopes in precipitation. Tellus 16, 436–468.

Dasgupta, R., 2013. Ingassing, Storage, and Outgassing of Terrestrial Carbon through Geologic Time. Rev. Mineral. Geochem. 75, 183–229. https://doi.org/10.2138/rmg.2013.75.7

Dasgupta, R., Hirschmann, M.M., 2010. The deep carbon cycle and melting in Earth's interior. Earth Planet. Sci. Lett. 298, 1–13. https://doi.org/10.1016/j.epsl.2010.06.039

Day, H.W., 2012. A revised diamond-graphite transition curve. Am. Mineral. 97, 52–62.

de Santis, R., Breedveld, G.J.F., Prausnitz, J.M., 1974. Thermodynamic properties of aqueous gas mixtures at advanced pressures. Ind. Eng. Chem. Process Des. Dev. 13, 374–377.

Duke, E.F., Rumble, D., 1986. Textural and isotopic variations in graphite from plutonic rocks, south-central New Hampshire. Contrib. Mineral. Petrol. 93, 409–419.

Evans, K., 2011. Metamorphic carbon fluxes: how much and how fast? Geology 39, 95–96.

French, B.M., 1966. Some geological implications of equilibrium between graphite and a C-H-O gas phase at high temperatures and pressures. Rev. Geophys. 4, 223–253.

Frost, B.R., 2018. Introduction to oxygen fugacity and its petrologic importance, in: Oxide Minerals. De Gruyter, pp. 1–10.

Galvez, M.E., Beyssac, O., Martinez, I., Benzerara, K., Chaduteau, C., Malvoisin, B. and Malavieille, J., 2013. Graphite formation by carbonate reduction during subduction. *Nature Geoscience*, *6*(6), pp.473-477.

Holloway, J.R., 1984. Graphite-CH4-H2O-CO2 equilibria at low-grade metamorphic conditions. Geology 12, 455–458.

Holloway, J.R., 1977. Fugacity and activity of molecular species in supercritical fluids, in: Thermodynamics in Geology. Springer, pp. 161–181.

Huang, F., Daniel, I., Cardon, H., Montagnac, G., Sverjensky, D.A., 2017. Immiscible hydrocarbon fluids in the deep carbon cycle. Nat. Commun. 8, 1–8.

Huizenga, J.M., 2005. COH, an Excel spreadsheet for composition calculations in the COH fluid system. Comput. Geosci. 31, 797–800.

Kendall, C., McDonnell, J.J., 2012. Isotope tracers in catchment hydrology. Elsevier Science Publishers: Amsterdam.

Kitchen, N.E., Valley, J.W., 1995. Carbon isotope thermometry in marbles of the Adirondack Mountains, New York. J. Metamorph. Geol. 13, 577–594.
Kokh, M.A., Akinfiev, N.N., Pokrovski, G.S., Salvi, S., Guillaume, D., 2017. The role of carbon dioxide in the transport and fractionation of metals by geological fluids. Geochim. Cosmochim. Acta 197, 433–466.
Luque, F.J., Crespo-Feo, E., Barrenechea, J.F., Ortega, L., 2012. Carbon isotopes of graphite: Implications on fluid history. Geosci. Front. 3, 197–207.
Mason, E., Edmonds, M., Turchyn, A.V., 2017. Remobilization of crustal carbon may dominate volcanic arc emissions. Science 357, 290–294.
Miozzi, F., Tumiati, S., 2020. Aqueous concentration of CO2 in carbon-saturated fluids as a highly sensitive oxybarometer. Geochem Persp Let 16, 30–34.
Ohmoto, H., Kerrick, D.M., 1977. Devolatilization equilibria in graphitic systems. Am. J. Sci. 277, 1013–1044.
Ortega, L., Millward, D., Luque, F.J., Barrenechea, J.F., Beyssac, O., Huizenga, J.-M., Rodas, M., Clarke, S.M., 2010. The graphite deposit at Borrowdale (UK): a catastrophic mineralizing event associated with Ordovician magmatism. Geochim. Cosmochim. Acta 74, 2429–2449.
Ray, J.S., 2009. Carbon isotopic variations in fluid-deposited graphite: evidence for multicomponent Rayleigh isotopic fractionation. Int. Geol. Rev. 51, 45–57.
Ray, J.S., Ramesh, R., 2000. Rayleigh fractionation of stable isotopes from a multicomponent source. Geochim. Cosmochim. Acta 64, 299–306.
Rayleigh, Lord, 1896. L. Theoretical considerations respecting the separation of gases by diffusion and similar processes. Lond. Edinb. Dublin Philos. Mag. J. Sci. 42, 493–498.
Richet, P., Bottinga, Y., & Javoy, M., 1977. A review of hydrogen, carbon, nitrogen, oxygen, sulphur, and chlorine stable isotope fractionation among gaseous molecules. *Annual Review of Earth and Planetary Sciences*, *5*(1), 65-110.
Rumble, D. and Hoering, T.C., 1986. Carbon isotope geochemistry of graphite vein deposits from New Hampshire, USA. *Geochimica et Cosmochimica Acta*, *50*(6), 1239-1247.
Sharp, Z., 2017. Principles of Stable Isotope Geochemistry, 2nd Edition. Pearson Prentice Hall. https://doi.org/10.25844/h9q1-0p82
Shi, P., Saxena, S.K., 1992. Thermodynamic modeling of the CHOS fluid system. Am. Mineral. 77, 1038–1049.
Spycher, N.F., Reed, M.H., 1988. Fugacity coefficients of H2, CO2, CH4, H2O and of H2O- CO2-CH4 mixtures: A virial equation treatment for moderate pressures and temperatures applicable to calculations of hydrothermal boiling. Geochim. Cosmochim. Acta 52, 739–749. https://doi.org/10.1016/0016-7037(88)90334-1
Stachel, T., Chacko, T., Luth, R.W., 2017. Carbon isotope fractionation during diamond growth in depleted peridotite: Counterintuitive insights from modelling water-maximum CHO fluids as multi-component systems. Earth Planet. Sci. Lett. 473, 44–51.
Stagno, V., Frost, D.J., 2010. Carbon speciation in the asthenosphere: Experimental measurements of the redox conditions at which carbonate-bearing melts coexist with graphite or diamond in peridotite assemblages. Earth Planet. Sci. Lett. 300, 72–84.
Taylor, B.E., Liou, J.G., 1978. The low-temperature stability of andradite in COH fluids. Am. Mineral. 63, 378–393.
Taylor, W.R., Green, D.H., 1986. The role of reduced COH fluids in mantle partial melting, in: International Kimberlite Conference: Extended Abstracts. pp. 211–213.
Tumiati, S., Recchia, S., Remusat, L., Tiraboschi, C., Sverjensky, D.A., Manning, C.E., Vitale Brovarone, A., Boutier, A., Spanu, D., Poli, S., 2022. Subducted organic matter buffered by marine carbonate rules the carbon isotopic signature of arc emissions. Nat. Commun. 13, 1–10.
Tumiati, S., Tiraboschi, C., Miozzi, F., Vitale-Brovarone, A., Manning, C.E., Sverjensky, D.A., Milani, S., Poli, S., 2020. Dissolution susceptibility of glass-like carbon versus crystalline graphite in

high-pressure aqueous fluids and implications for the behavior of organic matter in subduction zones. Geochim. Cosmochim. Acta 273, 383–402.
Ulmer, P., Luth, R.W., 1991. The graphite-COH fluid equilibrium in P, T, $$ f_ ${$O_2$}$ $$ space. Contrib. Mineral. Petrol. 106, 265–272.
Valley, J.W., 1986. Stable isotope geochemistry of metamorphic rocks. Rev. Mineral. Geochem. 16, 445–489.
Valley, J.W., O'Neil, J.R., 1981. 13C12C exchange between calcite and graphite: a possible thermometer in Grenville marbles. Geochim. Cosmochim. Acta 45, 411–419.
Vitale Brovarone, A., Tumiati, S., Piccoli, F., Ague, J.J., Connolly, J.A., Beyssac, O., 2020. Fluid-mediated selective dissolution of subducting carbonaceous material: Implications for carbon recycling and fluid fluxes at forearc depths. Chem. Geol. 549, 119682.

8 Supplementary material

Supplementary material 1:

The multicomponent model featured in tab 3 allows to monitor the isotopic evolution of a fluid containing both CO_2 and CH_4 in the case of precipitation of graphite/diamond. However, it does consider neither the mechanism, nor the thermodynamic settings linked to the precipitation. The Dissolution/precipitation model presented in tab 5 aims at coupling thermodynamic and isotopic evolutions. Here is a comparison of results provided by both methods from the modeling of desiccation of a fluid at CH_4/CO_2=0.9 at 800°C and 4 GPa (in the diamond stability field) from a fluid with an initial $\delta^{13}C$ composition of 0 ‰. Supplementary Figure 1 shows the results for each model, which are in excellent agreement

639 with each other. However, these methods can only be compared by desiccation process as
640 this is the only process supported by the multicomponent model.

641 Supplementary figure 1: Comparison of the diamond and fluid in the Thermotopes-COH
642 (TCOH) tab 5 Dissolution/precipitation and from the multicomponent system (MC). A:
643 Evolution of the $\delta^{13}C$ of diamond and fluid for each system as a function of the $CO_2/(CO_2+CH_4)$
644 ratio. B: Evolution of the Δ diamond-fluid for each system as a function of the $CO_2/(CO_2+CH_4)$
645 ratio.